

Wavelet Band Powers of the Primordial Power Spectrum from CMB Data

Pia Mukherjee, Yun Wang

Department of Physics & Astronomy, Univ. of Oklahoma, 440 W Brooks St., Norman, OK 73019

email: pia@nhn.ou.edu, wang@nhn.ou.edu

(November 11, 2018)

ABSTRACT

Measuring the primordial matter power spectrum is our primary means of probing unknown physics in the very early universe. We allow the primordial power spectrum to be an arbitrary function, and parametrize it in terms of wavelet band powers. Current cosmological data correspond to 11 such wavelet bands. We derive constraints on these band powers as well as H_0 , $\Omega_b h^2$ and $\Omega_m h^2$ from current Cosmic Microwave Background Anisotropy (CMB) data using the Markov Chain Monte Carlo (MCMC) technique. Our results indicate a feature in the primordial power spectrum at $0.008 \lesssim k/(h \text{ Mpc}^{-1}) \lesssim 0.1$. MAP and Planck data should allow us to put tighter constraints on the primordial power spectrum.

1. Introduction

As a result of recent cosmological data, inflation (Guth 1981; Albrecht & Steinhardt 1982; Gott 1982; Linde 1983) has become increasingly well established as the plausible solution to the problems of standard cosmology (Kolb & Turner (1990); see Peebles & Ratra (2003) for a recent review). The primordial power spectrum is our primary window into unknown physics during inflation (Wang, Spergel, & Strauss 1999; Chung et al. 2000; Enqvist & Kurki-Suonio 2000; Lyth, Ungarelli, & Wands 2002). It is of critical importance that we try to extract the primordial power spectrum, $P_{in}(k)$, from observational data without assuming specific forms for it.

Cosmological parameters are being measured to impressive precision with the help of recent CMB and large scale structure (LSS) data. The parameter constraints thus deduced are however sensitive to assumptions regarding the power spectrum of primordial density perturbations (Kinney (2001); Souradeep et al. (1998)). The primordial power spectrum is often assumed to be a power law, which represents many inflationary models (for example, see Linde (1983); Freese, Frieman, & Olinto (1990); La & Steinhardt (1991)). With such a parametrization the primordial power spectrum has been found to be scale invariant to a very good approximation, and its amplitude constrained (see for example Gorski et al. (1994); Lewis & Bridle (2002)). However, there are

many inflation models that predict primordial power spectra which cannot be parametrized by a simple power law (for example, Holman et al. (1991ab); Wang (1994); Randall, Soljagic, & Guth (1996); Adams, Ross, & Sarkar (1997); Lesgourgues, Polarski, & Starobinsky (1997); Lesgourgues (2000)). These can represent unusual physics in the very early universe. For example, inflation might occur in multiple stages in effective theories with two scalar fields (Holman et al. 1991ab), or in a succession of short bursts due to symmetry breaking during an era of inflation in supergravity models (Adams, Ross, & Sarkar 1997).

With the quality of data improving, more attention is being paid to the nature of the primordial perturbations (for example, see Covi, Lyth, & Melchiorri (2002); Leach & Liddle (2002)). As more observational data become available, they increase our ability to probe the primordial power spectrum, $P_{in}(k)$, as an arbitrary function of scale. A model independent determination of the $P_{in}(k)$ could uniquely probe physics of the very early universe, test what we have assumed about early universe physics, and provide powerful constraints on inflationary models. Wang, Spergel, & Strauss (1999) explored how this can be done with the CMB data from MAP¹ and LSS data from SDSS, using a piecewise constant function for $P_{in}(k)$. Wang & Mathews (2002) used the CMB data from Boomerang, Maxima, and DASI to place constraints on $P_{in}(k)$ using linear interpolation to approximate the function between several k values equally spaced in $\log k$.

Here we employ wavelets in a model independent parametrization of the primordial power spectrum and obtain constraints from current CMB data. We use only CMB data here, but LSS (for example, see Hamilton & Tegmark (2002); Percival et al. (2002); Bahcall et al. (2003)), and CMB polarization (for example, see Kovac et al. (2002)) data can all be added to help break or reduce degeneracies between different cosmological parameters and help better constrain $P_{in}(k)$.

We describe the wavelet parametrization of the primordial power spectrum in Sec.2 (see Appendix A for further discussion). In Sec.3, we discuss the techniques that we have used to optimize our method. Sec.4 contains our results. Sec.5 contains a summary and discussions.

2. Wavelet Band Powers of the Primordial Power Spectrum

Assuming that the primordial matter density fluctuations form a homogeneous Gaussian random field, the wavelet band powers of the primordial power spectrum $P_{in}(k)$, can be written as (see Eq.(A10))

$$P_j = \frac{1}{2^j} \int_{-\infty}^{\infty} dk \left| \hat{\psi} \left(\frac{k}{2^j} \right) \right|^2 P_{in}(k), \quad (1)$$

where $\hat{\psi}$ is the Fourier transform of the wavelet ψ (see Appendix A). P_j 's represent a scale-by-scale band averaged Fourier power spectrum, where the banding is not arbitrary but well defined, and naturally adaptive (as wavelets by construction afford better k resolution at smaller k). The P_j 's

¹<http://map.gsfc.nasa.gov/>

are mutually uncorrelated by construction (see Appendix A and Fang & Feng (2000) for further discussion of these issues).

To illustrate, Figure 1 shows a primordial power spectrum with features (solid line), similar to that discussed by Elgaroy, Gramann, & Lahav (2002). The points are the wavelet band powers P_j , computed using Eq.(1). These P_j 's can be thought of as being measured exactly from ideal data. Clearly, the wavelet band powers of the primordial power spectrum are excellent approximations of the primordial power spectrum at the central k values of the wavelet window functions, $\left|\hat{\psi}\left(\frac{k}{2^j}\right)\right|^2$ (dotted curves in Fig.1). Since the window functions are the modulus squared of the Fourier transform of dilations, by factors of 2, of the basic wavelet (see Appendix A), the peaks of these window functions are separated by factors of 2 in k . While we can add more bands to lower k , and 3 more bands at higher k that go up to 2π in k , and reconstruct the amplitude of the power in these additional bands, the locations of the bands or their widths cannot be changed. This is why in this scheme the banding is not arbitrary.

Hence we parametrize the primordial power spectrum $P_{in}(k)$ as follows [see Eq.(A11)]

$$P_{in}(k) = \sum_j P_j \left| \hat{\psi}\left(\frac{k}{2^j}\right) \right|^2. \quad (2)$$

The wavelet band powers P_j can be estimated from data that depend on the primordial power spectrum $P_{in}(k)$, for example, CMB and LSS data. Here we use only CMB data and estimate cosmological parameters together with the wavelet band powers P_j , which represent a measurement of the primordial power spectrum at the central k values of the wavelet window functions. P_j 's of unity corresponds to the default power of $A_s^2 = 2 \times 10^{-9}$, and if all P_j 's are set to unity we recover exactly the C_l spectrum that results from a scale invariant primordial power spectrum $P_s(k) = A_s^2 \left(\frac{k}{k_0}\right)^{n_s-1}$.

Figure 2 shows how each wavelet band power window function, $\left|\hat{\psi}\left(\frac{k}{2^j}\right)\right|^2$ [shown in Figure 1], maps on to a window function in the CMB angular power spectrum multipole number l space, for one set of cosmological parameters. These window functions have been numbered 7 to 17, which correspond to a range of $0.0001 \lesssim k/(h \text{ Mpc}^{-1}) \lesssim 0.5$. The 11 band powers, P_7 through P_{17} (from small to large k), are sufficient to constrain the primordial power spectrum from current and near future cosmological data. CMB data, up to an l_{max} of 1500, are insensitive to band powers P_1 to P_6 , which correspond to smaller k and have been set equal to P_7 , and to band powers higher than P_{17} , which correspond to larger k and have been set equal to P_{17} . The solid curve is the CMB angular power spectrum C_l that includes contributions from all the P_j 's [set to unity in this Figure]. Given that the CMB data are in the form of band powers in C_l s, and each multipole l maps on to a range in k (for example, see Figure 4 of Tegmark, & Zaldarriaga (2002)) with dependence on cosmological parameters, we see that in constraining P_j using cosmological data some correlations between the P_j 's will be inevitably introduced. The P_j 's are also correlated somewhat with the cosmological parameters in ways that can be understood from Figure 2.

For a comparison of different banding methods, instead of wavelet band powers we can parametrize the primordial power spectrum as a continuous and arbitrary function determined by its amplitude at several wavenumbers, equally spaced in $\log(k)$, using linear interpolation to approximate the function at intermediate wavenumbers. This is the linear interpolation binning method of Wang & Mathews (2002). In this work, we determine amplitudes at 11 wavenumbers corresponding to the central k values of the wavelet band powers. Figure 3 shows how each of these “binned” amplitudes map onto the CMB angular power spectrum multipole number l . The solid curve is the CMB angular power spectrum C_l with contributions from all the bins [all bin amplitudes set to 1]. The power in each bin, denoted here by a_j , is correlated with the power in neighboring bins from the start, and ultimately the resulting correlations will be different from the wavelet banding method. The error bars on the estimates will also be correlated. See Wang & Mathews (2002) for further details about this method.

3. Method

3.1. Optimization Techniques: Wavelet Projections and Markov Chain Monte Carlo

The usual approach to deriving cosmological constraints from CMB data is to grid over all the parameters being estimated and compute the likelihood at each point. Here, besides the 11 wavelet band powers (P_j ’s), we constrain H_0 , $\Omega_b h^2$ and $\Omega_c h^2$, assuming a flat universe with a cosmological constant Λ , and ignoring reionization and tensor modes. This results in 14 parameters. In order to place the most accurate and reliable constraint on the primordial power spectrum, we have chosen to compute the theoretical CMB angular power spectra at the accuracy of CMBFAST (Seljak & Zaldarriaga 1996) and CAMB (Lewis, Challinor, & Lasenby 2000). Our analysis would have been extremely time-consuming even on supercomputers. Fortunately, we are able to use two techniques which have made it possible for the analysis to be completed in a timely fashion.

First is the wavelet projections of the CMB angular power spectrum, C_l ’s. Using Eq. (2), we expand the CMB angular power spectrum as follows:

$$\begin{aligned} C_l(P_j, \mathbf{s}) &= (4\pi)^2 \int \frac{dk}{k} P_{in}(k) |\Delta_{Tl}(k, \tau = \tau_0)|^2 \\ &= \sum_j P_j \int \frac{dk}{k} \left| \hat{\psi} \left(\frac{k}{2^j} \right) \right|^2 |\Delta_{Tl}(k, \tau = \tau_0)|^2 \equiv \sum_j P_j C_l^j(\mathbf{s}), \end{aligned} \quad (3)$$

where the cosmological model dependent transfer function $\Delta_{Tl}(k, \tau = \tau_0)$ is an integral over conformal time τ of the sources which generate CMB fluctuations, τ_0 being the conformal time today, and \mathbf{s} represents the cosmological parameters other than the P_j ’s. We use CAMB² to compute the CMB angular power spectrum, in a form such that for given cosmological parameters other

²<http://camb.info/>

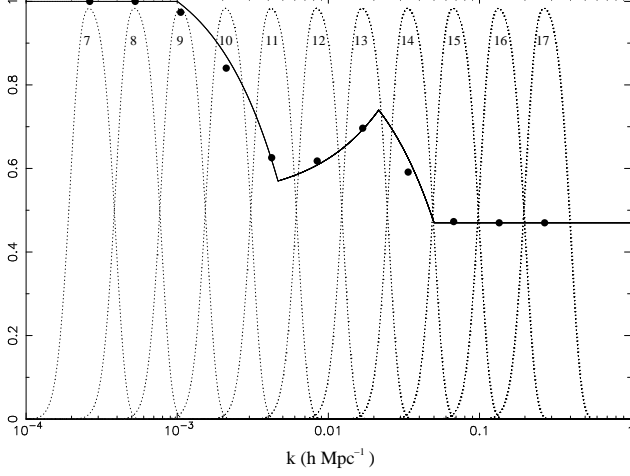


Fig. 1.— An example of a primordial power spectrum (solid line), and its wavelet band powers P_j 's ($j=7,17$; points), together with the corresponding wavelet window functions (dotted lines). The y axis is in arbitrary units.

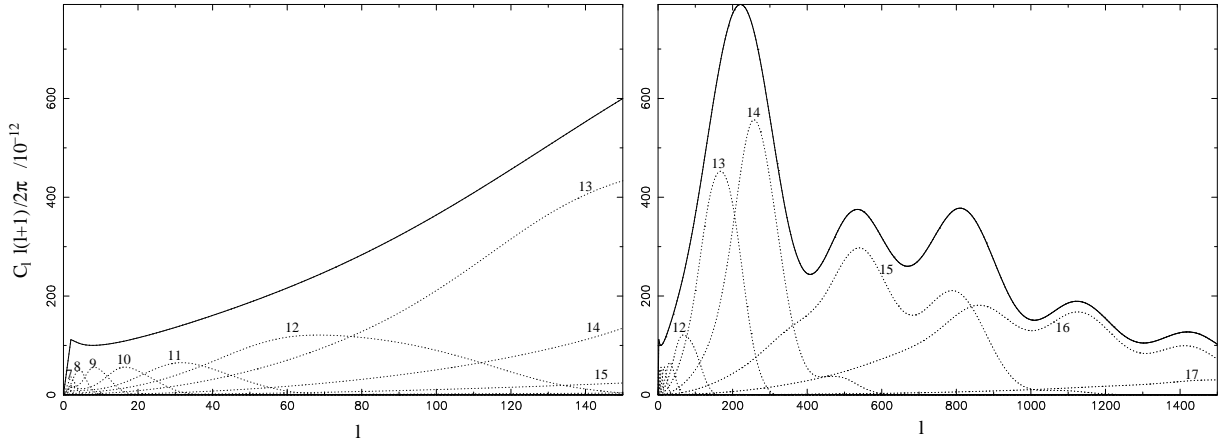


Fig. 2.— Mapping of the wavelet window functions of Figure 1 into window functions in the CMB multipole l space (dotted curves). The solid curve is the C_l spectrum that is the sum of contributions from all the wavelet bands (all the band powers, P_j , are set to unity here for illustration).

than the P_j 's, the $C_l^j(\mathbf{s})$ are computed, so that there is no need to call CAMB when we vary the P_j 's. This results in significant computational speed up. We expect this technique to be essential in constraining the primordial power spectrum with sufficient detail and speed.

The second technique is the Markov Chain Monte Carlo (MCMC) technique. The large number of parameters being varied here necessitates the use of this technique in the likelihood analysis. At its best, the MCMC method scales approximately linearly with the number of parameters. The method samples from the full posterior distribution of the parameters, and from these samples the marginalized posterior distributions of the parameters can be estimated. See Neil (1993) for a review, and Hannestad (2000); Knox et al. (2001); Lewis & Bridle (2002); Rubino-Martin et al. (2002) for applications of this method to CMB analysis.

3.2. Recipe for the Analysis

The steps followed in the analysis are as follows:

- (i) Establish the multi-dimensional parameter space that span all the parameters to be estimated from data. In our case, the total number of parameters is 14, including the wavelet band powers P_j 's.
- (ii) Start at some point in our 14d parameter space, which corresponds to an initial set of parameters. Note that the MCMC chain soon loses memory of this starting point and it can be verified that the result is independent of it.
- (iii) Find the likelihood of this set of parameter values given the data:

$$-2\ln(L) = \chi^2 \equiv \sum_{b,b'} \left[\ln(C_b + x_b) - \ln(C_b^{th} + x_b) \right] G_{b,b'} \left[\ln(C_{b'} + x_{b'}) - \ln(C_{b'}^{th} + x_{b'}) \right], \quad (4)$$

where C_b and C_b^{th} are the experimental and theoretically estimated band powers respectively, $G_{b,b'}$ is the corresponding band-band correlation matrix and x_b are the offset parameters in the offset-lognormal ansatz of Bond et al. (1998), or 0 for experimental results computed without this ansatz. For this purpose, we calculate the C_l spectrum for the given set of parameters, estimate the expected experimental band powers (for the given set of parameters) using the band power window functions available for the different CMB experiments, and compare these estimates to the measured band powers, taking into account the instrumental noise. We use offset-lognormal band-powers whenever available, and analytically marginalize over known beam and calibration uncertainties for each experiment, as described in Bridle et al. (2002).

- (iv) Take a random step in parameter space. The probability distribution of the step is taken to be Gaussian in each direction with an *rms* that is neither too small (or the chain will exhibit poor mixing) nor too large (or the chain efficiency will be poor). Ensure that the new point lies within the wide priors that define the likelihood region that one chooses to explore (our priors are defined in the next section). Calculate the likelihood at this new point (which corresponds to a new set of parameters).

(v) Use the Metropolis-Hastings algorithm (an MCMC sampler based on the Metropolis-Hastings algorithm has been made available in the software package CosmoMC (Lewis & Bridle 2002)) to determine whether to accept this point or to discard it and propose another point in the parameter space.

(vi) Repeat steps (iii) to (v) until a large number of samples from the posterior distribution of these parameters have been chosen.

(vii) Find the 1d marginalized parameter distributions and confidence limits for each parameter.

(viii) Check for convergence by running several chains starting at different initial values giving the same final distributions, and a couple of longer chains to ensure good sampling.

It would be interesting to include reionization and curvature in the analysis, and obtain additional constraints from different kinds of LSS data and ultimately also CMB polarization. We defer such extensions to the near future.

4. Results and Discussion

We use most of the recent high precision data for which experimental details are publicly available. These are the latest Boomerang (Ruhl et al. 2002), Maxima (Lee et al. 2001), DASI (Halverson et al. 2002), VSA (Scott et al. 2002), CBI (Pearson et al. 2002), ACBAR (Kuo et al. 2002) and Archeops (Benoit et al. 2002), together with COBE (Smoot et al. 1992). We estimate the wavelet band powers of the primordial power spectrum, as well as H_0 , $\Omega_b h^2$ and $\Omega_c h^2$.

All results shown in this paper are for the wavelet Daubachies 20 [see Appendix A].

Allowing all 14 parameters to vary, the results obtained are shown in Figure 4. We have used a weak prior of the age of the universe $t_0 > 10$ Gyrs. All the P_j 's are consistent with unity at $\sim 1.5\sigma$. However, there is some indication of a feature in $P_{in}(k)$, though at low significance. Figure 4 shows that current CMB data seem to favor a dip at a k of $\sim 0.01 h \text{ Mpc}^{-1}$ (from P_{12}) and excess power k of ~ 0.02 to $0.03 h \text{ Mpc}^{-1}$ (from P_{13} and P_{14}), followed by another small dip from P_{16} at k of $\sim 0.1 h \text{ Mpc}^{-1}$. The cosmological parameters are constrained to $h = 0.56 \pm 0.09$, $\Omega_b h^2 = 0.020 \pm 0.005$ and $\Omega_c h^2 = 0.161 \pm 0.028$.^{3, 4} Note that the derived value of the Hubble constant

³In this paper we quote the mean of the derived 1d distributions, instead of the maximum, for the constrained parameters, following Lewis & Bridle (2002). As discussed in Lewis & Bridle (2002), the MCMC samples from the posterior do not provide accurate estimates of parameter best-fit values, because in higher dimensions the best-fit region typically has a much higher likelihood than the mean but occupies a minuscule fraction of parameter space. Our main results are not affected by this.

⁴This corresponds to $\Omega_b = 0.062[0.048, 0.079]$ and $\Omega_c = 0.51[0.42, 0.60]$. Note the degeneracies between the cosmological parameters considered here. Due to the geometrical degeneracy, the location of the first acoustic peak nails the curvature of the universe (here taken to be zero) but a degeneracy between Ω_m and Ω_Λ , or equivalently Ω_m and h remains. The height of the first peak is degenerate for $\Omega_b h^2$ and $\Omega_c h^2$. Precise determination of the second and third peak heights can help determine $\Omega_b h^2$ and thus ease degeneracies (for example, see Efstathiou & Bond

h is lower than the value of h derived assuming a scale-invariant primordial power spectrum (i.e., setting all the P_j 's to the same constant value). Assuming scale-invariance gives $h = 0.71 \pm 0.06$, $\Omega_b h^2 = 0.023 \pm 0.001$, $\Omega_c h^2 = 0.122 \pm 0.016$ and all P_j 's = 0.90 ± 0.06 . A chi square analysis indicates that a model with the P_j 's estimated from data (i.e., allowing $P_{in}(k)$ to be a free function) and the best fit scale invariant model (setting all P_j 's equal to a constant) fare about the same. For a low h , the derived Ω_m is high. If we used an external constraint, such as from LSS, to keep Ω_m low, the derived h would be higher; this is a result of parameter degeneracies in CMB data.

Figure 5 shows the CMB power spectrum corresponding to the fitted cosmological parameters and P_j 's and also the CMB power spectrum for the same cosmological parameters but with all P_j 's set to unity. One can see where the P_j 's are contributing. Most distinctly, by allowing the P_j 's to vary, the CMB angular power spectrum receives significant positive contribution around the first peak.

The corresponding results for the case of the linear interpolation binning method are in Figure 6. Note that the primordial power spectrum reconstructed in this way is consistent with the primordial power spectrum reconstructed using wavelet band powers [Figure 4]. This is reassuring since in the two methods the parameters being reconstructed have different correlations amongst themselves and with the other cosmological parameters [see Figures 2 and 3]. The bin amplitudes a_1 to a_6 do not rule out the excess power at small k that was found by Wang & Mathews (2002). But from the marginalized distributions we see that these bin amplitudes are not constrained and vary over the entire range that was allowed in the runs. In comparison the wavelet banding method works better. This is as expected since the wavelet band powers are uncorrelated by construction, hence are less correlated when estimated from data than the linear interpolation bins.

Now we examine the effect, on the wavelet band power results, of imposing statistical priors. If a Gaussian prior is introduced in the value of h , a weak conservative prior of 0.6 ± 0.1 (Branch 1998), together with the above mentioned weak age prior, what results is almost identical to Figure 4. If a stronger prior on h is introduced, that of $h = 0.72 \pm 0.08$ (Freedman et al. 2001) we find that the feature in the $0.008 \lesssim k/(h \text{ Mpc}^{-1}) \lesssim 0.1$ range remains, though it reduces in amplitude as a whole by nearly 10% (Figure 7). Cosmological parameters are simultaneously constrained to be $h = 0.64 \pm 0.06$, $\Omega_b h^2 = 0.023 \pm 0.004$ and $\Omega_c h^2 = 0.147 \pm 0.022$. Note that when the P_j 's were varied near the currently favored values of the cosmological parameters ($h = 0.68$, $\Omega_b h^2 = 0.024$, and $\Omega_c h^2 = 0.12$), the same form for the primordial power spectrum, with the whole spectrum shifted down by about 20%, was obtained. Without priors on the Hubble constant, the current CMB data seem to prefer a somewhat low Hubble constant of $h = 0.56 \pm 0.09$ with the freedom that is allowed in the shape of the primordial power spectrum. It is not clear whether this is due to any systematic effects. Note that however, this lowish value of the Hubble constant is within the uncertainties of other independent measurements of H_0 (for example, see Branch (1998); Freedman et al. (2001); Gott et al. (2001); Saha et al. (2001)).

(1999); Hu et al. (2001); White & Cohn (2002)).

We note that several other groups have studied the constraint on specific types of features of the primordial power spectrum from current observational data; our findings are consistent with these results (Silk, & Gawiser 2000; Atrio-Barandela et al. 2001; Barriga et al. 2001; Hannestad, Hansen, & Villante 2001; Elgaroy, Gramann, & Lahav 2002).

The advantage of our approach in this paper versus previous work is as follows. We parametrize the primordial power spectrum by its wavelet band powers P_j . This is a model independent parametrization of $P_{in}(k)$ ⁵. Wang, Spergel, & Strauss (1999) parametrize the primordial power spectrum by a step function [i.e., top-hat banding]; this leads to an estimated primordial power spectrum $P_{in}(k)$ that is *discontinuous*, while the $P_{in}(k)$ estimated using wavelet band powers is *continuous*. Wang & Mathews (2002) used linear interpolation of $P_{in}(k)$ values at several k values [equally spaced in $\log k$]; this lead to a continuous estimated $P_{in}(k)$, but the $P_{in}(k)$ values estimated from data are strongly correlated. The wavelet band powers P_j are mutually uncorrelated by construction [see Eqs.(1)(2), though some correlations are inevitably introduced because the data that are used to constrain them are bands in l space], and the banding in this method is not arbitrary. Note also that by computing the wavelet projections of C_l [see Eq.(3)] for each set of cosmological parameters excluding the P_j 's, we avoid computing C_l when we vary the wavelet band powers P_j in the likelihood analysis. This, together with the MCMC technique, made it possible for us to estimate all the 11 relevant wavelet band powers from the current CMB data in a timely fashion. We expect that our method will be efficient in yielding tighter and detailed constraints on $P_{in}(k)$ when applied to MAP and Planck data.

Finally we note that the primordial power spectrum results presented here are for k in units of $h \text{ Mpc}^{-1}$. These units are found to yield more constraining results and this is important for pre-WMAP data. Some published results are for $P_{in}(k)$ with k in units of Mpc^{-1} . Note that when $P_{in}(k)$ is given with k in units of Mpc^{-1} , the feature we have found in this paper would be shifted to smaller k , to near $k \sim 0.01 \text{ Mpc}^{-1}$.

5. Conclusions

A model independent determination of the $P_{in}(k)$ could uniquely constrain unknown physics in the very early universe, test what we have assumed about early universe physics, and provide powerful constraints on inflationary models. Thus rather than assuming specific forms for $P_{in}(k)$, we have used a wavelet band power expansion to extract $P_{in}(k)$ as a free function, using recent high precision CMB data. The wavelet band powers parametrization of the primordial power spectrum has the following features: in this scheme the banding is not arbitrary but well defined and adaptive. In terms of these band powers the primordial power spectrum can be reconstructed as a smooth function. The band powers are mutually uncorrelated by construction, and they are excellent

⁵Miller et al. (2002) do a model independent analysis of the CMB angular power spectrum C_l 's.

approximations of the primordial power spectrum at the central k value of the wavelet window functions. Although in estimating these from CMB data, which are band powers in multipole space, some correlations are inevitably introduced because of the cosmological model dependent nonlinear mapping between wavenumber k and multipole l spaces.

The wavelet band powers of $P_{in}(k)$ that we have extracted from current CMB data seem to indicate a feature in the primordial power spectrum at $0.008 \lesssim k/(h \text{ Mpc}^{-1}) \lesssim 0.1$, though only at low significance. A chi square analysis indicates that a model with the estimated P_j 's and cosmological parameters and the best fit scale invariant model fare about the same. Future data will better help distinguish between these models. The linear interpolation binning approach of Wang & Mathews (2002) yields an estimated $P_{in}(k)$ with a similar feature at roughly the same location in k with comparable significance. Our results are consistent with previous work by Wang & Mathews (2002). MAP and Planck⁶ data should allow us to put a tighter constraint on the primordial power spectrum (Lesgourgues, Prunet, & Polarski 1999; Wang, Spergel, & Strauss 1999; Hannestad 2001; Matsumiya, Misao Sasaki, & Yokoyama 2002; Tegmark, & Zaldarriaga 2002).

We acknowledge the use of CAMB and CosmoMC. This work was supported by NSF CAREER grant AST-0094335 at the Univ. of Oklahoma. We thank the referee for helpful comments.

REFERENCES

- Adams, J.A., Ross, G.G., & Sarkar, S. 1997, Nuclear Physics B, 503, 405
- Albrecht, A., Steinhardt, P. J. 1982, Phys. Rev. Lett., 48, 1220
- Atrio-Barandela, F., Einasto, J., Mller, V., Mcket, J. P., Starobinsky, A. A. 2001, ApJ, 559, 1
- Bahcall, N.A. et al. 2003, ApJ, in press, astro-ph/0205490
- Barriga, J., Gaztanaga, E., Santos, M., Sarkar, S. 2001, MNRAS, 324, 977
- Benoit, A., et al. 2002, submitted to A&A Letter, astro-ph/0210305
- Bond, J.R., Jaffe, A.H., & Knox, L.E. 2000, ApJ, 533, 19
- Branch, D. 1998, ARA&A, 36, 17
- Bridle, S. et al. 2002, MNRAS 335, 1193
- Burles, S., Nollett, K.M., & Turner, M.S. 2001, ApJ, 552, 1
- Chung, D.J.H., Kolb, E.W., Riotto, A., Tkachev, I.I. 2000, Phys. Rev. D, 62, 043508

⁶<http://astro.estec.esa.nl/Planck/>

- Covi, L., Lyth, D.H., Melchiorri, A. 2002, hep-ph/0210395
- Daubechies, I. 1992, Ten Lectures on Wavelets, S.I.A.M., Philadelphia.
- Efstathiou, G., Bond, J. R. 1999, MNRAS, 304, 75
- Elgaroy, O., Gramann, M., Lahav, O. 2002 MNRAS, 333, 93
- Enqvist, K., & Kurki-Suonio, H. 2000, Phys. Rev. D, 61, 043002
- Fang, L.Z., & Feng, L.L. 2000, ApJ, 539, 5
- Frazier, M., Jawerth, B. & Weiss, G. 1991, *Littlewood-Paley Theory and the Study of Function Spaces*. American Mathematical Society.
- Freedman, W. L. et al. 2001, ApJ, 553, 47
- Freese, K., Frieman, J.A., & Olinto, A.V. 1990, Phys. Rev. Lett., 65, 3233
- Gorski, et al. 1994, ApJ, 430, L89
- Gott, J. R. 1982, Nature, 295, 304
- Gott, J. R., Vogeley, M. S., Podariu, S., Ratra, B. 2001, ApJ, 549, 1
- Guth, A.H. 1981, Phys. Rev. D, 23, 347
- Halverson, N.W., et al. 2002, ApJ, 568, 38
- Hamilton, A.J.S., Tegmark, M. 2002, MNRAS, 330, 506
- Hannestad, S. 2001, Phys.Rev. D, 63, 043009
- Hannestad, S, Hansen, S.H., Villante, F.L. 2001, Astropart.Phys. 16, 137
- Hannestad, S. 2000, Phys.Rev. D61, 023002
- Holman, R., Kolb, E.W., Vadas, S.L., & Wang, Y. 1991a, Phys. Rev., D43, 3833
- Holman, R., Kolb, E.W., Vadas, S.L., & Wang, Y. 1991b, Phys. Lett., B269, 252
- Hu, W., Fukugita, M., Zaldarriaga, M., & Tegmark, M. 2001, ApJ, 549, 669
- Kinney, W. H. 2001, Phys.Rev. D63, 043001
- Knox, L., Christensen, N., & Skordis, C. 2001, ApJ, 563, L95
- Kolb, E.W., & Turner, M.S. 1990, *The Early Universe* (Addison-Wesley Publishing Company)
- Kovac, J. et al. 2002, astro-ph/0209478

- Kuo, C.L., et al. 2002, submitted to ApJ, astro-ph/0212289
- La, D., & Steinhardt, P.J. 1991, Phys. Rev. Lett., 62, 376
- Leach, S.M., & Liddle, A.R. 2002, astro-ph/0207213
- Lee, A.T., et al. 2001, ApJ, 561, L1
- Lesgourgues, J., Polarski, D., & Starobinsky, A.A. 1997, Nuclear Physics B, 497, 479
- Lesgourgues, J., Prunet, S., & Polarski, D. 1999, MNRAS, 303, 45
- Lesgourgues, J. 2000, Nucl. Phys. B582, 593
- Lewis, A., Challinor, A., & Lasenby, A. 2000, ApJ, 538, 473, astro-ph/9911177
- Lewis, A., & Bridle, S. 2002, astro-ph/0205436
- Linde, A.D. 1983, Phys. Lett., 129B, 177
- Lyth, D. H., Ungarelli, C., & Wands, D. 2002, Phys Rev D in press, astro-ph/0208055
- Matsumiya, M., Sasaki, M., & Yokoyama, J. 2002, Phys.Rev. D, 65, 083007
- Miller, C.J., Nichol, R.C., Genovese, C., & Wasserman, L. 2002, ApJ, 565, L67
- Mukherjee, P., Hobson, M., & Lasenby, A. 2000, MNRAS, 318, 1157
- Neil, R.M. 1993, <ftp://ftp.cs.utoronto.ca/pub/radford/review.ps.gz>
- Pearson, T.J., et al. 2002, submitted to ApJ, astro-ph/0205388
- Peebles, P.J.E., & Ratra, B. 2003, RMP, in press, astro-ph/0207347
- Percival, W.J. et al. 2002, MNRAS, in press, astro-ph/0206256
- Press, W.H., Teukolsky, S.A., Vetterling, W.T., & Flannery, B.P. 1994, Numerical Recipes, Cambridge University Press, Cambridge.
- Randall, L., Soljadic, M., & Guth, A. 1996, Nucl. Phys. B472, 377
- Rubino-Martin, J.A., et al. 2002, submitted to MNRAS, astro-ph/0205367
- Ruhl, J.E., et al. 2002, astro-ph/0212229
- Saha, A. et al. 2001, ApJ, 562, 314
- Scott, P.F., et al. 2002, astro-ph/0205380
- Seljak, U., & Zaldarriaga, M. 1996, ApJ, 469, 437

- Silk, J., & Gawiser, E. 2000, *Physica Scripta* T85, 132 (2000)
- Smoot, G.F., et al. 1992, *ApJ*, 396, L1
- Souradeep, T., Bond, J.R., Knox, L., Efstathiou, G., & Turner, M.S. 1998, in *Proceedings of COSMO-97*, Ambleside, England, ed. L. Roszkowski, World Scientific (astro-ph/9802262)
- Tegmark, M., & Zaldarriaga, Z. 2002, *Phys.Rev. D*, 66, 103508
- Tenorio, L., Jaffe, A., Hanany, S. & Lineweaver, C.H. 1999, *MNRAS*, 310, 823
- Tenorio, L., Stark, P. & Lineweaver, C.H. 1999, *Inverse Problems*, 15, 329
- Walter, G.G. 1992, *Wavelets and other Orthogonal Systems with Applications*, CRC Press
- Wang, Y. 1994, *Phys. Rev.*, D50, 6135
- Wang, Y., Spergel, D.N., and Strauss, M.A. 1999, *ApJ*, 510, 20
- Wang, Y., & Mathews, G. J., *ApJ*, 573, 1
- White, Martin, & Cohn, J. D. 2002, *AmJPh*, 70, 106
- Zhang, J. & Walter, G.G. 1994, *IEEE Trans. Sig. Proc.*, 42, 1737

A. Wavelet Band Powers

Here we describe our wavelet parametrization of the primordial power spectrum in detail.

The wavelet transform bases are obtained from dilations and translations of a certain (mother) function $\psi(x)$ via

$$\psi_{j,l}(x) = \left(\frac{2^j}{L}\right)^{1/2} \psi(2^j x/L - l). \quad (\text{A1})$$

where $\psi(x)$ is in general real, defined on the interval $[0, 1]$, and obeys several restrictive mathematical relations first derived by Daubechies (1992) in order for the resulting wavelet basis to be discrete, orthogonal and compactly-supported. These are the kind of wavelets we consider here. See, for example, Press et al. (1994) for an introduction to wavelets, and Barreiro et al. (2000) and Tenorio et al. (1999) for applications of spherical wavelets to CMB data on the sky. The j and l are scale and position indices respectively, and the wavelet bases are orthogonal with respect to both these indices,

$$\int_{-\infty}^{\infty} \psi_{j,l}(x) \psi_{j',l'}(x) dx = \delta_{jj'} \delta_{ll'}.$$

A periodic function $f(x)$ of period L , sampled at $N = 2^J$ equally spaced points between 0 and L , can be expanded in terms of the wavelet basis as

$$f(x_i) = \sum_{j=0}^{J-1} \sum_{l=0}^{2^j-1} b_{j,l} \psi_{j,l}(x_i), \quad (\text{A2})$$

where the coefficients $b_{j,l}$ are given by

$$b_{j,l} = \int_0^L f(x) \psi_{j,l}(x) dx. \quad (\text{A3})$$

The scale index j increases from 0 to $J - 1$, and the wavelets with increasing j represent the structure in the function on increasingly smaller scales, with each scale a factor of 2 finer than the previous one. The index l (which runs from 0 to $2^j - 1$) denotes the position of the wavelet $\psi_{j,l}$ within the j th scale. Thus $b_{j,l}$ measures the signal in $f(x)$ on scale $L/2^j$, and centered at position $lL/2^j$ in physical space and centered at wavenumber $2\pi \times 2^j/L$ in Fourier space.

The Fourier decomposition of function $f(x_i)$ is given by

$$f(x_i) = \sum_{n=0}^{N-1} \epsilon_n e^{i2\pi n x_i/L} \quad (\text{A4})$$

and the Fourier coefficient ϵ_n is

$$\epsilon_n = \frac{1}{L} \int_0^L f(x) e^{-i2\pi n x/L} dx. \quad (\text{A5})$$

Since both the discrete wavelet transform (DWT) and the Fourier transform (FT) bases are complete, there exists a relationship between the Fourier and wavelet coefficients. Substituting equation (A4) in (A3) gives

$$b_{j,l} = \sum_{n=-\infty}^{\infty} \epsilon_n \hat{\psi}_{j,l}(-n), \quad (\text{A6})$$

and similarly equations (A5) and (A2) give

$$\epsilon_n = \frac{1}{L} \sum_{j=0}^{\infty} \sum_{l=0}^{2^j-1} b_{j,l} \hat{\psi}_{j,l}(n), \quad (\text{A7})$$

where $\hat{\psi}_{j,l}(n)$ is the FT of the wavelet $\psi_{j,l}$ and is related to the FT of the basic wavelet (using (A1)) by

$$\hat{\psi}_{j,l}(n) = \int_0^L \psi_{j,l}(x) e^{-i2\pi nx/L} dx = \left(\frac{2^j}{L}\right)^{-1/2} \hat{\psi}\left(\frac{n}{2^j}\right) e^{-i2\pi nl/2^j}. \quad (\text{A8})$$

From (A6), the covariance in wavelet space is given by

$$\langle b_{j,l} b_{j',l'} \rangle = \sum_{n,n'=-\infty}^{\infty} \langle \epsilon_n, \epsilon_{n'} \rangle \hat{\psi}_{j,l}(n) \hat{\psi}_{j',l'}^\dagger(n'). \quad (\text{A9})$$

For a homogeneous Gaussian random field, ignoring the often very small correlations that may exist between the wavelet coefficients (see Frazier, Jawerth & Weiss (1991), Walter (1992), Zhang & Walter (1994), and Tenorio, Stark & Lineweaver (1999); such correlations, ignored in mosts works, reduce further with the regularity of the wavelet), $\langle b_{j,l} b_{j',l'} \rangle = P_j \delta_{j,j'} \delta_{l,l'}$.⁷ Also for a Gaussian random field the Fourier amplitudes ($|\epsilon_n|$) have a Gaussian one point distribution and their phases are random, so that $\langle \epsilon_n, \epsilon_{n'} \rangle = P(n) \delta_{n,n'}$. Thus

$$P_j = \frac{1}{2^j} \sum_{n=-\infty}^{\infty} \left| \hat{\psi}\left(\frac{n}{2^j}\right) \right|^2 P(n). \quad (\text{A10})$$

where P_j is the variance of $b_{j,l}$, the power of perturbations in wavelet coefficients of scale j .

The P_j 's are thus the scale-by-scale band-averaged Fourier power spectrum, from which one can attempt to reconstruct the Fourier power spectrum as a smooth function. The weak correlation of the wavelet coefficients discussed above leads to an excellent approximation to $P(n)$:

$$\hat{P}(n) = \sum_{j=0}^{\infty} P_j \left| \hat{\psi}\left(\frac{n}{2^j}\right) \right|^2. \quad (\text{A11})$$

⁷When the random field is ergodic, the 2^j coefficients at a given scale can be taken as 2^j independent measurements. The average over l is thus a fair estimation of the ensemble average.

Moreover, for a Gaussian random field the P_j 's are (very nearly, see discussion above) uncorrelated:

$$\frac{\langle P_j P_{j+1} \rangle}{P_j P_{j+1}} = \frac{2^{j+1} \sum_l b_{j,l/2}^2 b_{j+1,l}^2}{\sum_l b_{j,l/2}^2 \sum_l b_{j+1,l}^2} = 1. \quad (\text{A12})$$

Scale-scale correlations, as defined above for order 2 (the value of the exponent), has been discussed in detail by Pando, Valls-Gabaud & Fang (1998), and Mukherjee, Hobson & Lasenby (2000), and others (note that there are half the number of coefficients at scale j than at scale $j + 1$). The existence of detectable scale scale correlations is an indication of mode-mode coupling and hence non-Gaussianity.

In order to parametrize the primordial power spectrum in a model independent way, we need to estimate the power in certain bands in k . The bands should be logarithmically spaced in k , as in Wang & Mathews (2002). To find a unique number for the appropriate number of bands to use, we adopt the DWT approach to banding. While in the Fourier approach the phase space is split such that the resolution in wavenumber k is highest at all k ($\Delta k \rightarrow 0$), and the resolution in position x is lowest, ($\Delta x \rightarrow \infty$), in the wavelet approach these resolutions are adaptive. We choose $\Delta x \propto 1/k$, and $\Delta k/k = \log 2$, so that an optimal chopping of the phase space is achieved whilst satisfying the uncertainty relation $\Delta x \Delta k \geq 2\pi$ (see Fang & Feng (2000) for a discussion). Wavelets afford good k resolution at small k and poorer resolution by factors of 2 as j (or position resolution) increases. Further, the wavelet band powers P_j , for a Gaussian random field, are uncorrelated by definition, and one cannot have more independent bands (Fang & Feng 2000). Equations (A10) and (A11) show how the primordial Fourier power spectrum can be parametrized in terms of P_j 's which represent a scale-by-scale band-averaged Fourier power spectrum with $\log_{10}(2)$ spacing.

Note the Eq.(A10) is essentially just a suitable form of banding with window functions shown in Fig. 1. The equations preceding it in this section show that if the field in question, here a statistically homogeneous and isotropic Gaussian random primordial density field, were available to us then the P_j 's would be the variance of wavelet coefficients of scale j . Although we have given equations for a 1d field, if the primordial density field is isotropic the equivalence can be made.

All results shown in this paper are for the wavelet Daubachies 20. We have also studied the case for the Symmlet 8 wavelet, obtaining very similar results. The larger the number associated with the wavelet, the more smooth is the wavelet in real space, and the lesser their compact support in real space (less localized, though compact support is technically more involved a concept than localization, and while wavelets can be localized in both real and Fourier space, it is impossible for a function to have compact support in both spaces). Since we hope to be able to pick up sharp features in the primordial (Fourier) power spectrum, wavelets that are smooth in real space are preferable for our purpose. In fact wavelets that have compact support in Fourier space rather than in real space (often called band-limited wavelets) should do better. Examples of such wavelets are the Shannon wavelet and the Meyer wavelet. We defer their use for a future paper as these are less frequently used wavelets so that the relevant software is not easily available.

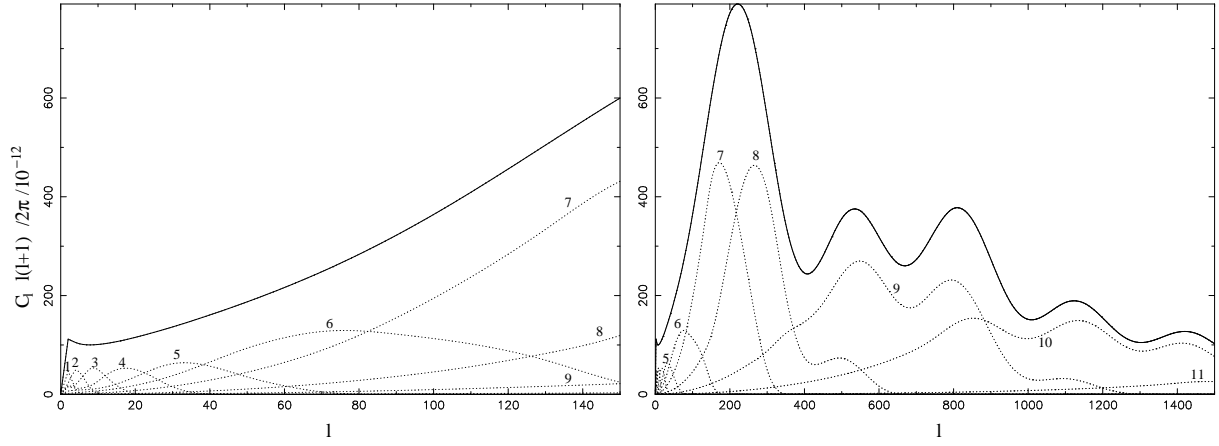


Fig. 3.— Mapping of an arbitrary number of bins, here chosen to be 11, to correspond exactly to the central k values of the 11 wavelet bands discussed above, into window functions in the CMB multipole l space (dotted curves). The solid line is the C_l spectrum that includes contributions from all the bins (all the bin amplitudes are set to unity here for illustration).

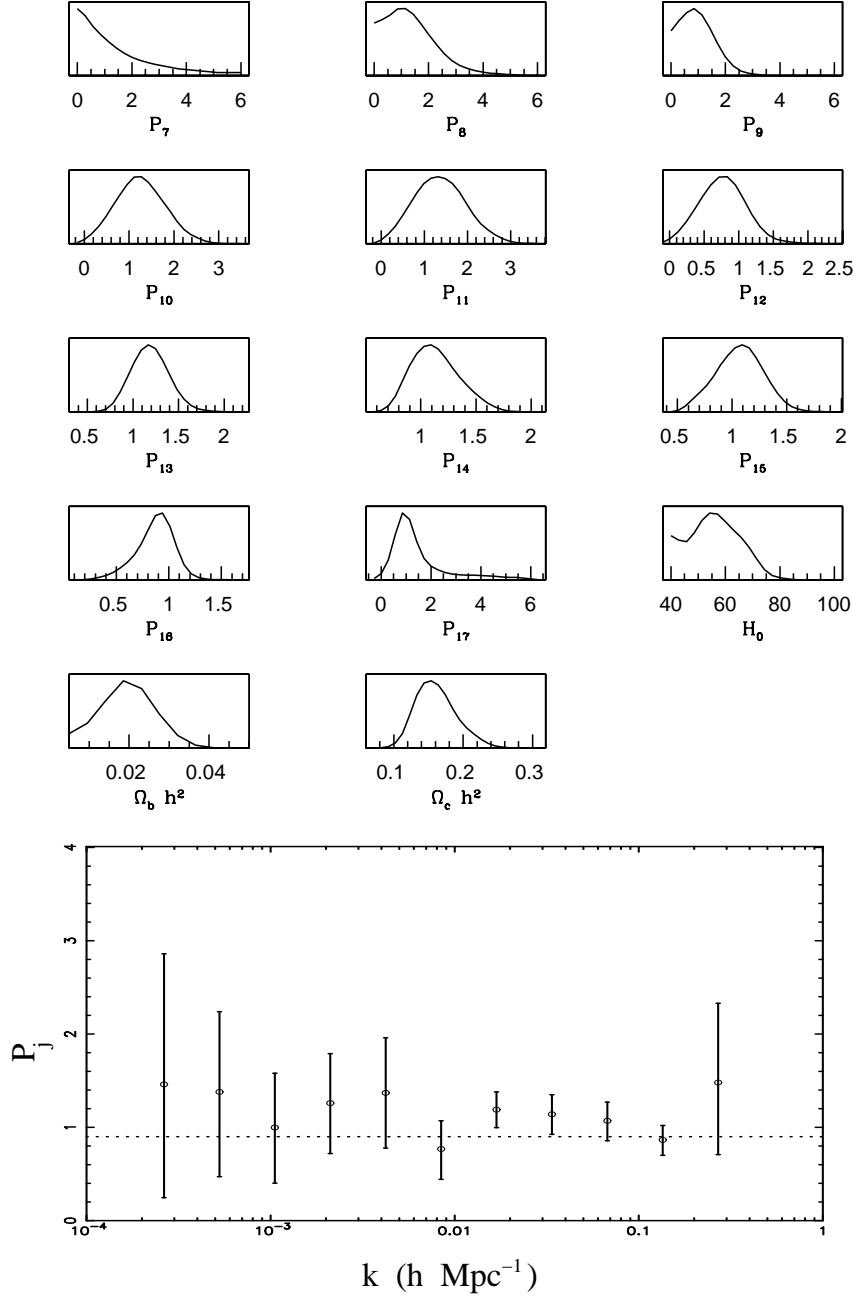


Fig. 4.— The 1d marginalized posterior distributions obtained upon varying all the 14 parameters. The bottom plot shows the constrained P_j 's (j=7,17) versus scale. The dotted line indicates the best-fit scale-invariant model. The cosmological parameters are simultaneously constrained to be $h = 0.56 \pm 0.09$, $\Omega_b h^2 = 0.020 \pm 0.005$ and $\Omega_c h^2 = 0.161 \pm 0.028$.

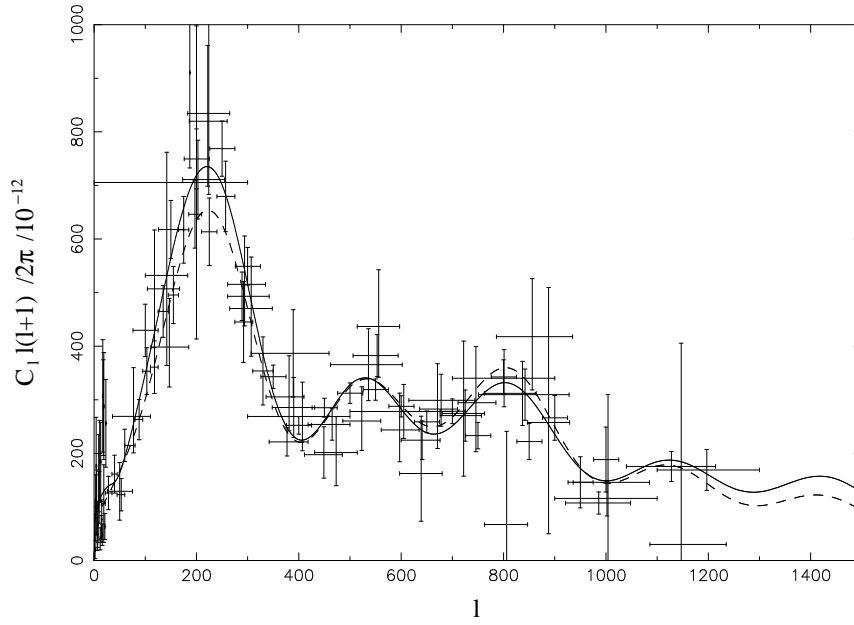


Fig. 5.— The solid line shows the CMB power spectrum at fitted values of the cosmological parameters and P_j 's. The dashed line shows the CMB power spectrum for the same cosmological parameters at P_j 's of unity. All the data points considered in the analysis are plotted. The error bars do not include calibration and beamwidth uncertainties.

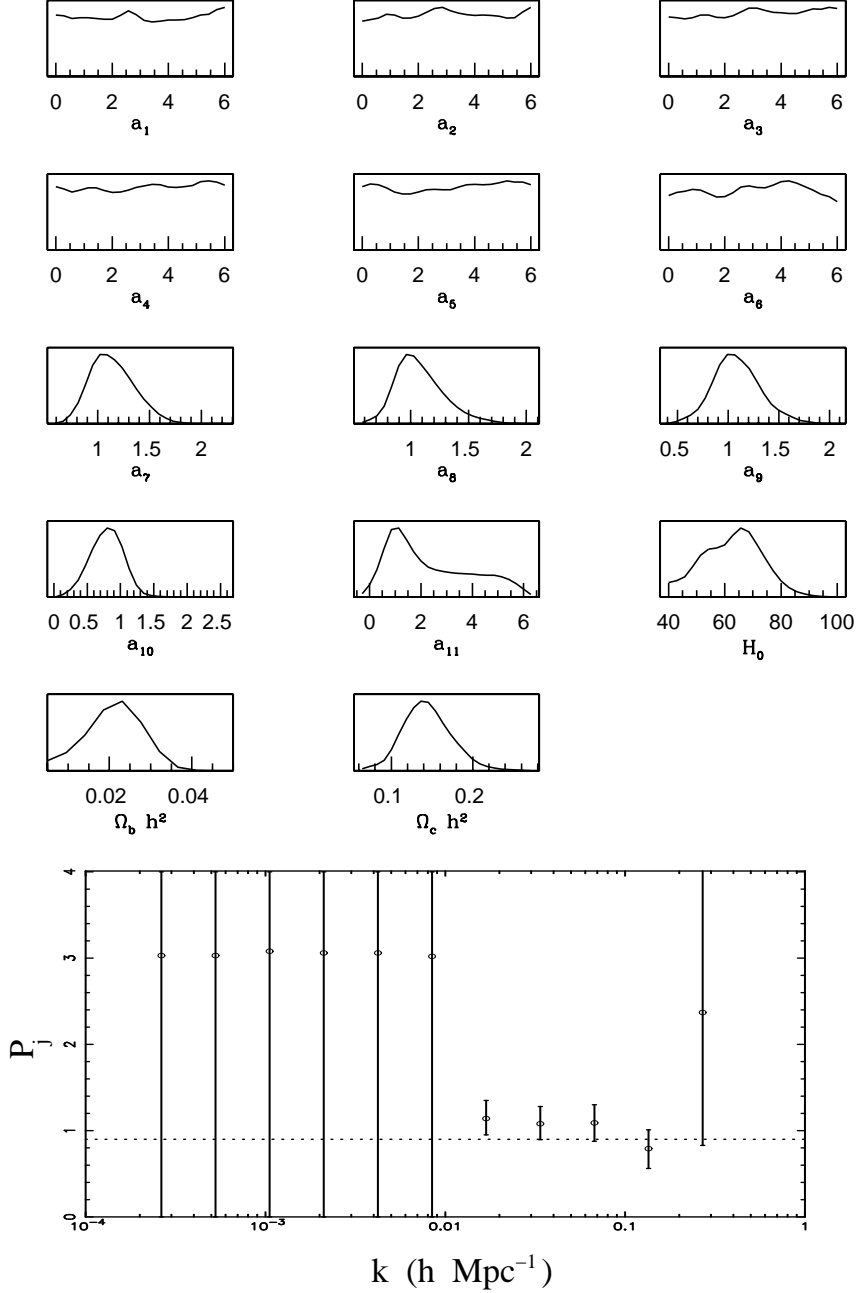


Fig. 6.— Results obtained by parameterizing the primordial power spectrum with bin amplitudes a_j s in 11 bins ($j=1,11$) corresponding exactly to the central k values of the wavelet bands. The dotted line indicates the best-fit scale-invariant model. The amplitudes a_1 to a_6 are unconstrained; hence their standard deviation is not meaningful. The cosmological parameters are simultaneously constrained to be $h = 0.63 \pm 0.10$, $\Omega_b h^2 = 0.021 \pm 0.005$ and $\Omega_c h^2 = 0.144 \pm 0.029$.

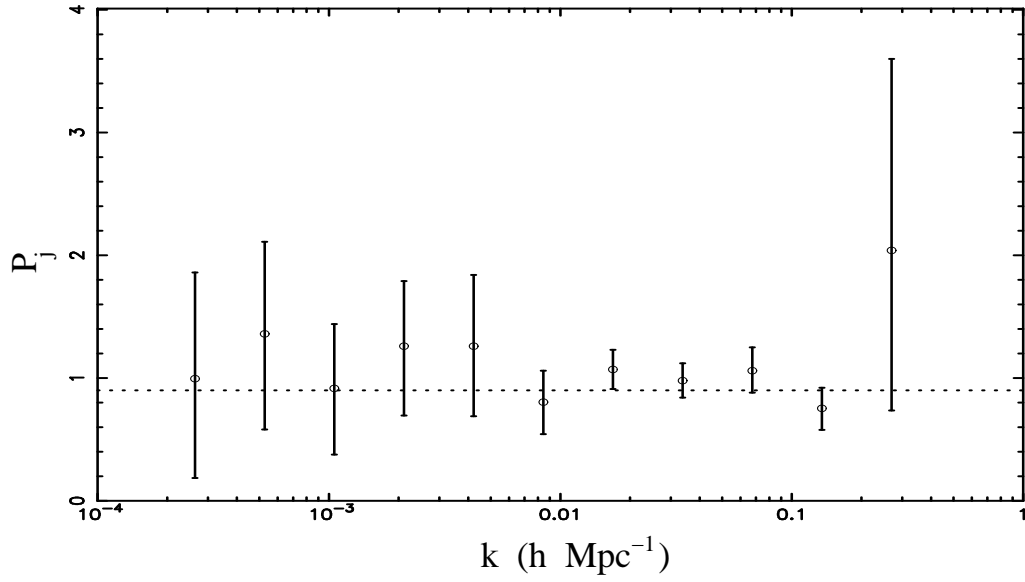


Fig. 7.— Same as Figure 4, but with a strong prior on H_0 (see text). The cosmological parameters are simultaneously constrained to be $h = 0.64 \pm 0.62$, $\Omega_b h^2 = 0.021 \pm 0.004$ and $\Omega_c h^2 = 0.144 \pm 0.022$.